Stanford Exploration Project, Report 102, October 25, 1999, pages 1–14

Common-azimuth migration of a North Sea dataset

Louis Vaillant and Paul Sava[1]

keywords: *3-D prestack depth migration, common-azimuth, velocity estimation, common-image gathers*

ABSTRACT

3-D prestack common-azimuth depth migration has a strong potential for imaging accurately complex media and handling multi-pathing. We apply the technique to North Sea real data for imaging a salt dome. The results obtained demonstrate the efficiency of the method in complex media. A detailed analysis of common-image gathers shows opportunities for improving the velocity model.

INTRODUCTION

Wave-equation migration techniques have benefited from a renewed interest now that some shortcomings of Kirchhoff migration have been highlighted (O'Brien and Etgen, 1998). Moreover, intensive computing resources now make 3-D prestack depth migration feasible with such techniques. Based on a recursive extrapolation of the recorded wavefield, wave-equation migration methods are potentially better able to handle multi-pathing problems induced by complex velocity structures. Thus, they offer an attractive alternative to Kirchhoff methods (Mosher et al., 1997; Biondi, 1997). Moreover, wave propagation is modeled out of the asymptotic approximation context.

Common-azimuth migration (Biondi and Palacharla, 1996) is a 3-D prestack depth migration technique based on the wave equation. It exploits the intrinsic narrow-azimuth nature of marine data to reduce its dimensionality and thus manages to cut the computational cost of 3-D imaging significantly. In this paper, we discuss the first application of this imaging technique to real data at SEP. For this purpose, Elf Aquitaine provided us with an interesting dataset recorded in the North Sea, which shows a salt dome and other 3-D structures. The complexity of the wave propagation in the medium, resulting from high velocity contrasts (lateral and longitudinal), yields multi-pathing and illumination problems, which makes this model both a serious challenge for imaging and an interesting test case for the common-azimuth migration.

[1]**email:** louis@sep.stanford.edu, paul@sep.stanford.edu

DATA CHARACTERISTICS AND PROCESSING

Figure 1 shows a section of a velocity model created from our real dataset. It illustrates the most important interfaces and the lithology of the medium. This section has been used to generate finite-difference synthetic data by Elf Aquitaine in cooperation with IFP[2] and has proved to be a test case for imaging below salt flanks (Prucha et al., 1998; Malcotti and Biondi, 1998). The geologic interpretation proposed by IFP comes from the analysis of the real dataset. This geologic model will be referred to regularly in this paper.

The recorded data covers an area of 13.5×4km for a whole volume of seismic information as big as 45 gigabytes. The first step of our processing was to perform a gridding of the whole volume and then to apply a simple sequence NMO/binning/NMO^{-1} for regularizing the data. As a first approach to the imaging problem, we stacked the data and migrated them using a 3-D zero-offset extended split-step algorithm (Stoffa et al., 1990). In order to get these preliminary results more quickly, we used this first migrated cube to extract a subset (Figure 1) from the whole data, which includes most target regions of interest, such as the top of salt and the salt flanks.

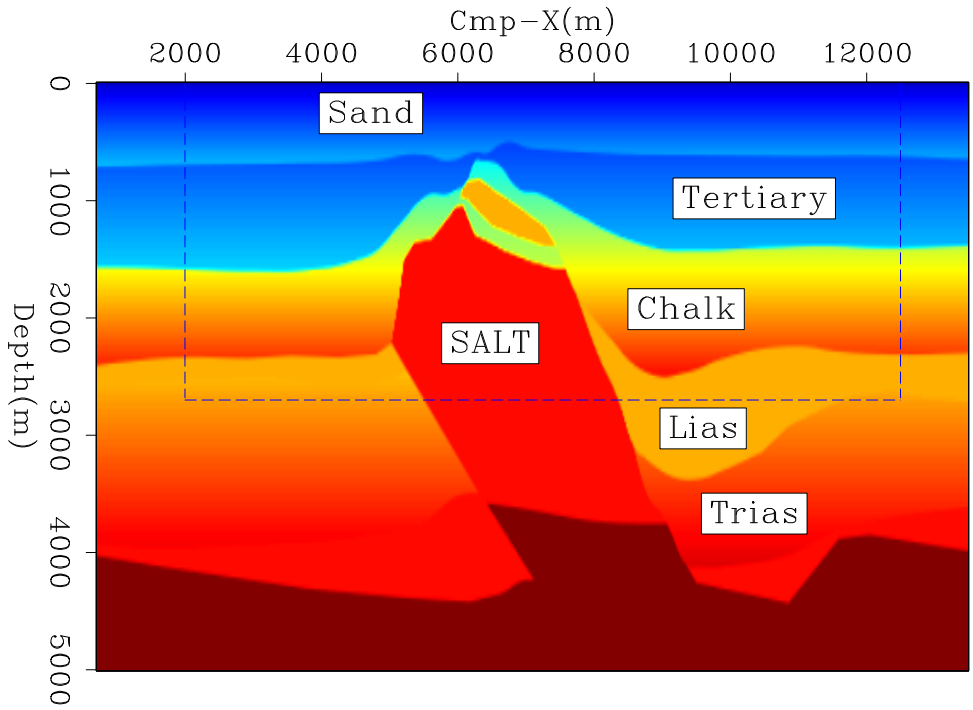

Figure 1: Synthetic velocity model elaborated from the North Sea data, with its lithology. The dashed box represents the subset migrated in this study. louis1-L7d-vel-synth [CR]

Because we wanted to examine how robust the method was with respect to lateral velocity variations, both in the cross-line and the in-line direction, we kept all the data along the Cmp-Y axis. By resampling the data in Cmp-X and in offset (Table 1) at the limit of aliasing, we

[2]Institut Français du Pétrole

reduced the cube dimension to less than 20 gigabytes, which is more reasonable costwise. From now on, “data” will always refer to this particular subset.

One could object that the most important imaging challenge for this particular model would be to focus the base of salt accurately, since it probably corresponds to the most complex propagation for the wavefield through the body itself. However, we chose not to image all the way down in this first test in order to limit the computational time. We also focused on improving the velocity model in the upper part. This choice helps us image deeper regions accurately, as we will see in the last sections of the paper.

	Cmp-X range	Cmp-X sampling	Cmp-Y range	Cmp-Y sampling	Offset range	Offset sampling
Raw data	0-13500 m	13.33 m	1600-5600 m	25.0 m	185-3570 m	25 m
Subset	2000-12500 m	20.0 m	1600-5600 m	25.0 m	200-3400 m	50 m

Table 1: Geometrical characteristics of the selected data

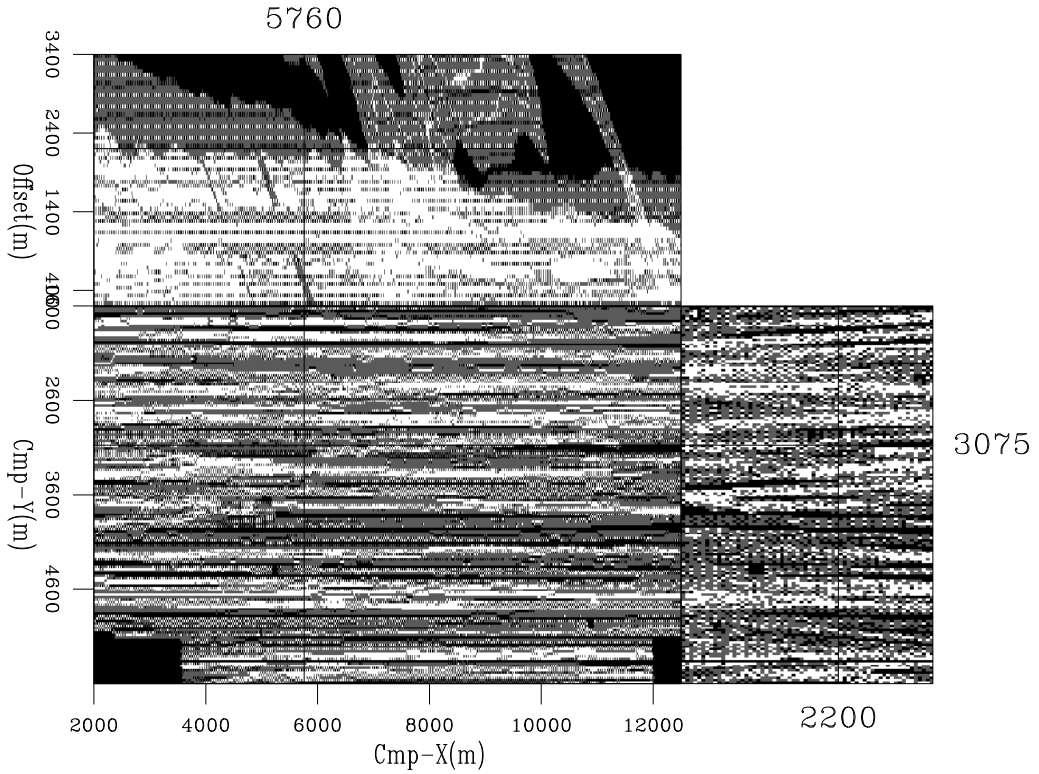

Figure 2: 3-D fold map of the data gridded with the parameters presented in Table 1. “Black” is zero-fold, and “white” corresponds to 8 traces per bin. louis1-L7d-subset-fold [CR]

After this gridding, the data shows an irregular repartition, especially on Cmp-X vs. offset planes (Figure 2). Apparently, several geophones in the middle of the streamers went down

during the acquisition, which yields a very irregular fold for the binning and large areas with no offset information.

Azimuth moveout (Biondi et al., 1998) is the operator usually used for transforming the data to common-azimuth and putting them on a regular grid. We estimated that performing AMO on our data would need 7 days of computation, which is not negligible compared to the cost of the migration itself (see paragraph below). Since the data were concentrated in a narrow azimuth band, we instead used a simple binning procedure, normalized by the fold. AMO will be used for a further comparison in the near future.

The common-azimuth data obtained by NMO/binning/NMO^{-1} were migrated down to 2700m, with a depth spacing of 12.5m. We used 6 reference velocities for the extended split-step scheme that performs migration. With the dimensions indicated in Table 2, the 3-D prestack common azimuth migration ran in 26 days on 4 processors of our SGI Power Challenge (18 MIPS R8000 Processors, 2 Gbytes of memory). To put this in context, the zero-offset migration took about 12 hours on only 2 processors of the same machine.

	Number of samples					
	Cmp-X	Cmp-Y	Depth	Offset	Frequencies	Velocities
Subset	525	160	216	64	150	6

Table 2: Dimensions of the data and migration quantities

COMMON-AZIMUTH IMAGING RESULTS

Figure 3 shows a typical set of sections in the middle of the migrated cube. In the in-line section, the shallower part down to 1500m reveals high frequency details accurately imaged. The migration enhanced a graben structure, with normal faults and rocked blocks, around location Cmp-X=8000m, close to the top in the sand layer. The most energetic interfaces in the section, located approximately at depth 1500m, correspond to the limit tertiary/chalk in the geologic interpretation presented in Figure 1. The velocity model indicates a strong velocity contrast there, with more than 1000m/s difference between the two media.

The horizontal section at depth 900m highlights complex patterns inside the tertiary layer, imaged with a high resolution. Those can be interpreted as turbidite channels. The main direction of slumping is along the in-line, away from the salt dome. We can infer as a hypothesis that the upcoming salt may be the cause of the flow and of the resedimentation.

Both the depth section and the cross-line section show an oblique fault through the chalk layer just above the salt body. On one side of the fault inside the chalk appears a strong reflector, like a block of salt separated from the main body, or perhaps another lithologic feature. The bottom interface of the chalk layer with the Lias is imaged accurately.

The salt body in itself is well delimited on its right side. The top-left boundary is well focused after migration, though with a weaker amplitude. Although we can observe the sediments in the chalk bent upwards by the upcoming salt on the left-hand side, the boundary itself

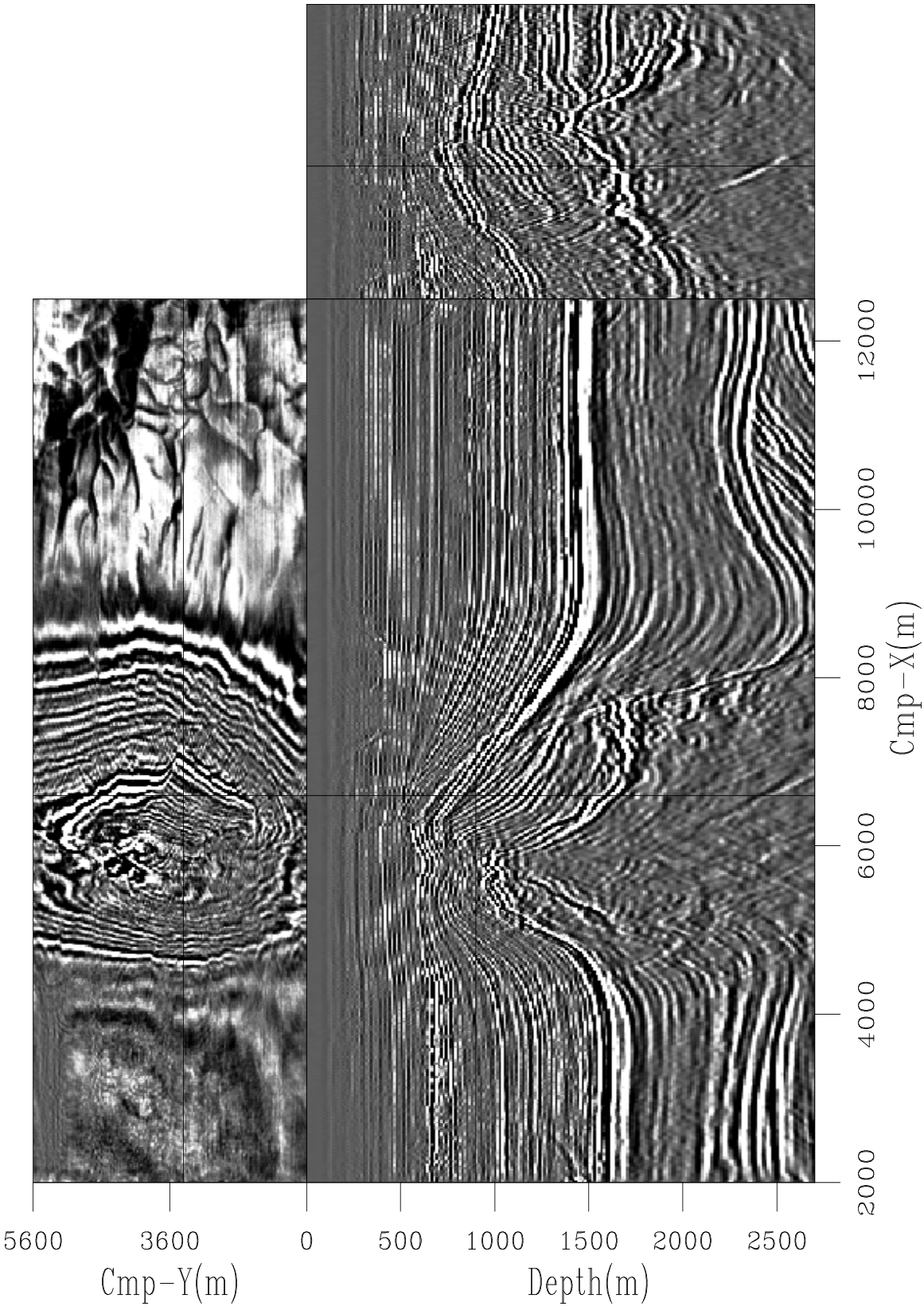

Figure 3: Sections of the migrated data at location: depth=900m, Cmp-X=6600m, Cmp-Y=3400m. louis1-L7d-ComAz-mig-all [CR]

is not clearly recovered by the migration. We expect it to be almost vertical, with the beginning of the overhang below depth 2500m. In the cross-line direction, the top of salt reveals a complex shape, as seen in that section. The imaging there seems satisfactory, and the top of salt is quite continuous.

Seismic imaging can be sketched as a two-step process: velocity estimation and migration. All modern migration algorithms require a simple and reliable way to extract prestack information for velocity estimation and updating. For this purpose, 3-D angle-domain common-image gathers can be easily computed in the wavenumber domain from the output of common-azimuth migration (Prucha et al., 1999; Sava, 1999). Those panels enhance valuable information for analysis when the velocity model is complex and induces multi-pathing.

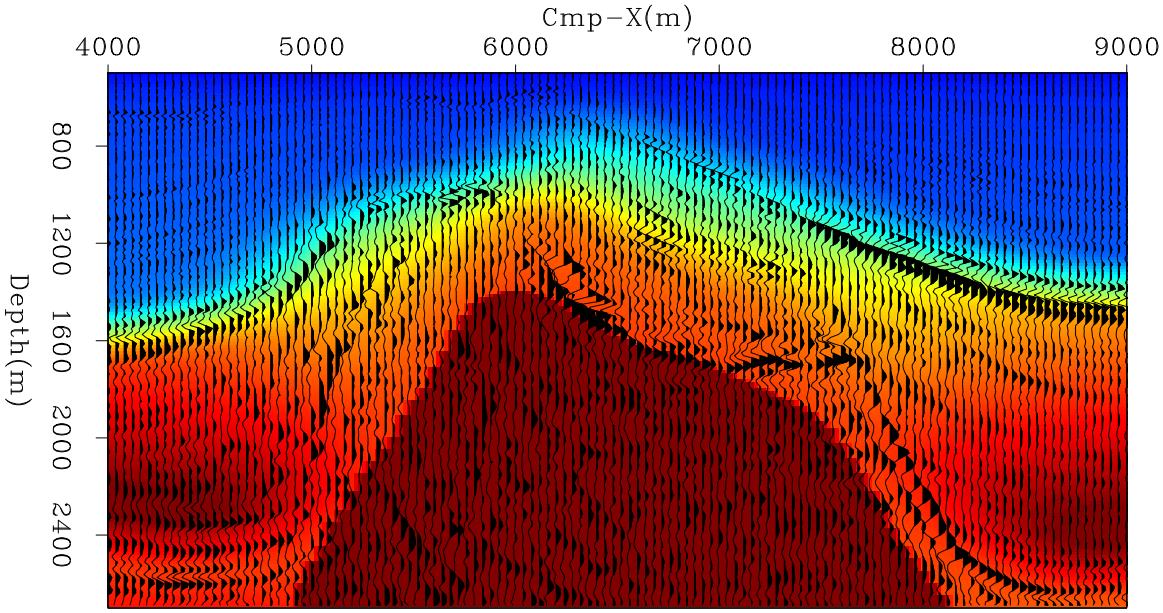

Figure 4: Close-up of the salt body. The near-angle migrated section has been superimposed on the velocity model. louis1-L7d-ysect1-and-vel [CR]

Figure 5 shows the same in-line section as before (Cmp-Y=3400m), with examples of the angle-domain common-image gathers that can be obtained from the migrated image. Unlike the image in figure 3, the section is not a stack over the angle axis but instead a near-angle image. Even if it increases the noise level, it also displays more events that are not stacked coherently because the velocity is not perfect. For the sake of clarity, we will next focus on this particular in-line section and will use it as a support for the analysis of our migration results.

In figure 5, panels (a) and (b) show that the reflectors corresponding to the interface Tertiary/salt are well aligned along the angle axis. Similarly, in panel (c), the complex interface chalk/Lias/Trias at the bottom-right of the section reveals flat gathers. The velocity at these interfaces is well determined. The top and the left-hand side of the salt body (panels (a) and (b)) are not perfectly flattened in the gathers. The inclusion labeled “I” above the salt that causes an energetic reflection yields a slightly high velocity anomaly since it is not accounted for in the velocity model (see figure 4).

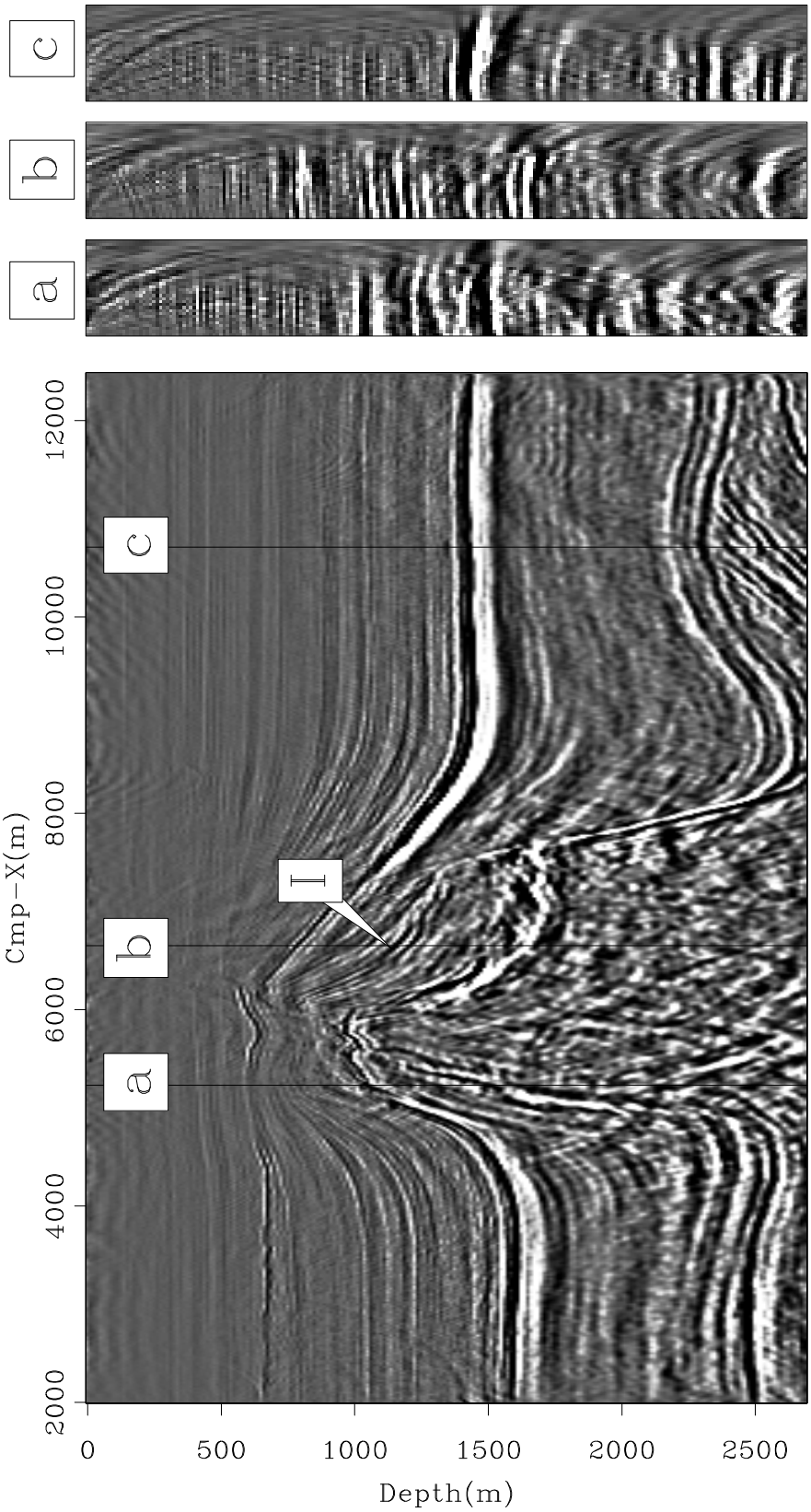

Figure 5: In-line near-angle section at location Cmp-Y=3400m and several angle-domain common-image gathers (a), (b) and (c) louis1-L7d-ang-ysect1-set1 [CR]

DISCUSSION

The velocity model we used for the migration was obtained by reflection tomography using the S.M.A.R.T[3] method (Jacobs et al., 1992; Ehinger and Lailly, 1995). We smoothed their result before running the common-azimuth migration. Our smoothing scheme preserved the exact shape of the salt body to avoid high velocity spreading into the surrounding model, which would degrade imaging.

Figure 6 shows common-image gathers along our main in-line section, illustrating details of the salt boundaries. When searching for these boundaries on the left-hand side, the event marked "R" seems relatively coherent compared to the ratio of noise that can be observed inside the salt. It may reasonably correspond to the salt flank we hope to image on the left-hand side. The event could as well be an internal multiple created by reflections on Tertiary/chalk or chalk/salt interfaces around event "I". Additionally, Ogilvie and Purnell (1996) show how converted waves can also create spurious events sufficiently high in amplitude to confound interpretation.

If "R" is effectively the salt flank, its location after migration remains inaccurate, since we would expect it to be immediately against the reflectors bending upwards in the chalk. This event possibly comes from a wavefield seriously distorted while traveling through the salt body and recorded at large Cmp-X locations. In contrast, the salt boundary closer to the top is better migrated since the waves have not propagated through the dome and have instead been recorded at small Cmp-X locations. Panel (a) illustrates this hypothesis, showing flat gathers for the top of the salt edge and, below, reflectors bending upwards with angle around reflector "R".

Furthermore, panels (b) and (c) intersect an area where the continuity of the salt top is broken. At this particular location, the zero-offset migration, being less sensitive to velocity variations, yields more continuous imaging (Figure 7). The common-image gathers show reflectors bending upwards, indicating a too low velocity. Similarly, on the right-hand side, the salt flank shows a too low velocity (panel (d)).

We can see from the analysis of common-image gathers that the velocity model obviously needs further improvements. Figure 4 shows the salt boundaries in the migrated section superimposed on the velocity model we used for imaging. Performing accurate imaging, especially deeper in the model, requires a more precise relocation of the major reflectors, such as the salt edges, with respect to the velocity model.

For this purpose, the information provided by the common-image gathers can be reinvested in a residual migration process to improve the focusing of the migrated sections. The next step, which is less straightforward, is to update the velocity model from the perturbation between the starting and the improved images (Biondi and Sava, 1999). This remains an open research subject.

Last, we compare the result of 3-D prestack common-azimuth migration with the 3-D

[3]Sequential Migration-Aided Reflection Tomography - KIM (Kinematic Inversion Methods), IFP consortium

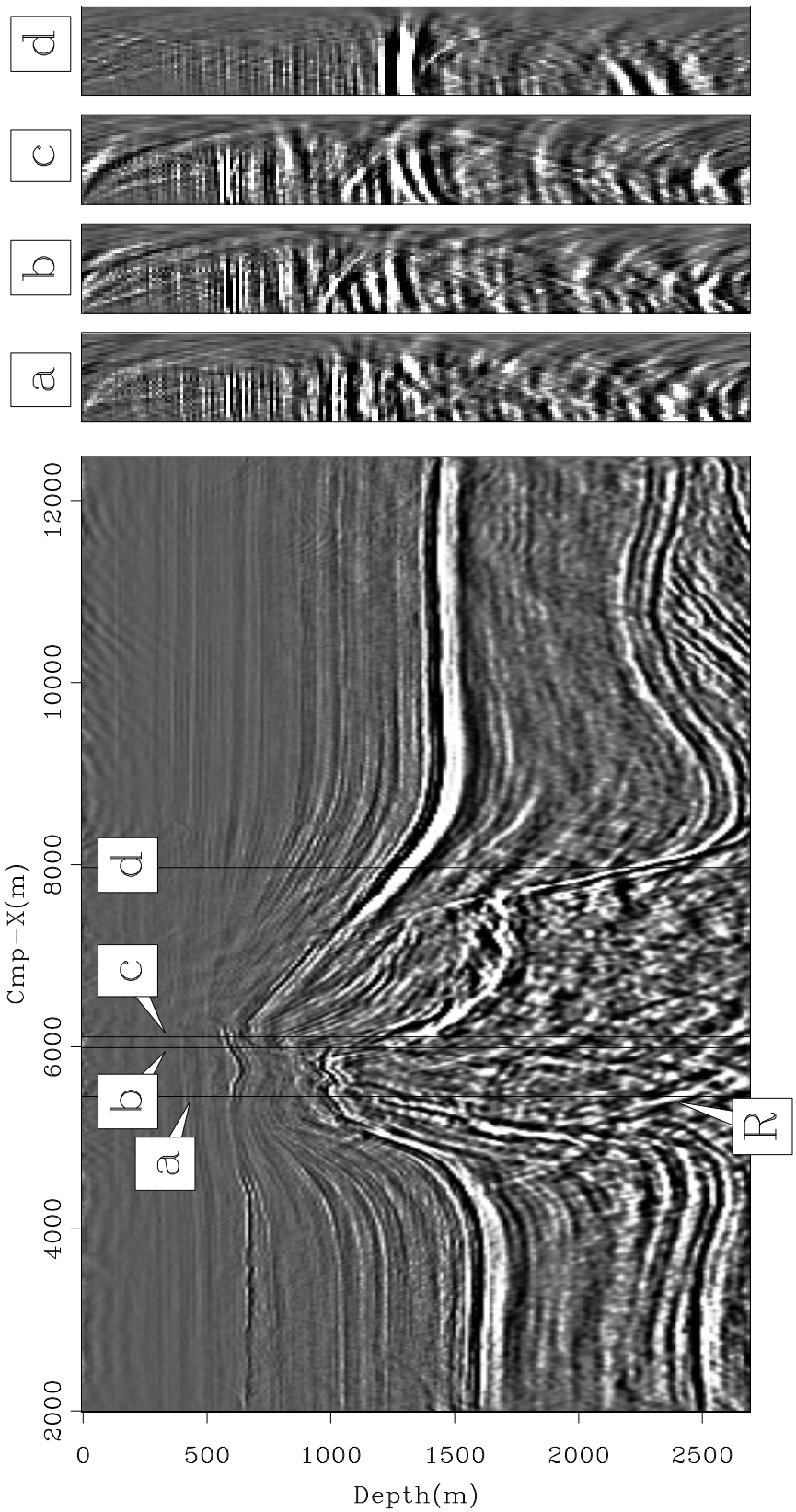

Figure 6: In-line near-angle section at location Cmp-Y=3400m with angle-domain common-image gathers louis1-L7d-ang-ysect1-set2 [CR]

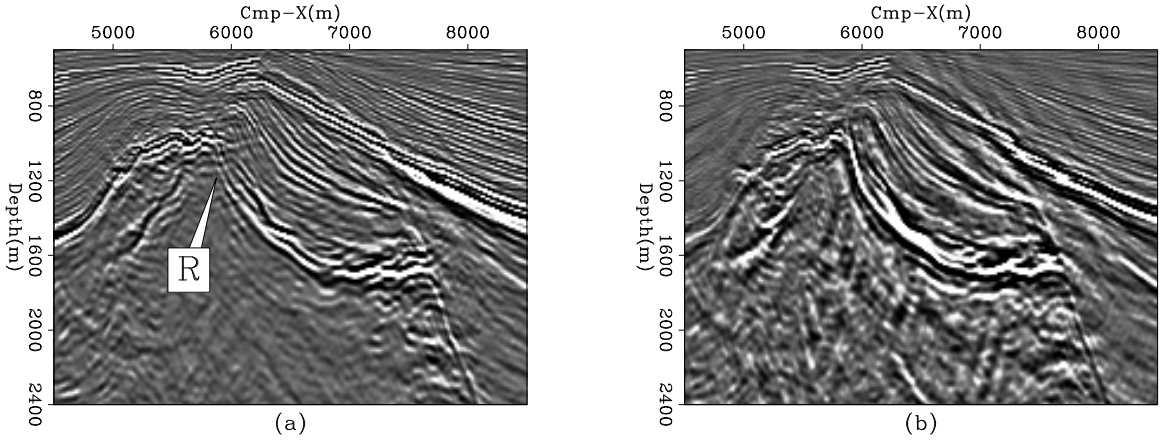

Figure 7: Close-up of the salt dome for the common-azimuth migrated image (a) and the section migrated with zero-offset extended split-step algorithm (b). "R" points out the reflector of interest. The clip percentile is the same on both images (96). louis1-L7d-salt-ComAz-and-ZOmig [CR]

prestack preserved-amplitude depth migration (PAPsDM) result, courtesy of the Ecole des Mines de Paris (Xu et al., 1999). Figure 8 shows both results, which are derived from the same velocity model. However, their implementation of the ray+Born formalism (Thierry et al., 1999a,b) for elaborating the PAPsDM algorithm yields an image in impedance perturbation rather than in reflectivity (as in the case of 3-D prestack common-azimuth migration). In order to make the migrated images more comparable, we differentiated their result along the depth axis. Although this conserves the shapes of the reflectors, the conversion to reflectivity implies (in theory) differenting perpendicularly to the reflectors, which is not straightforward.

Both sections (a) and (b) in figure 8 display many similarities. The sides of the salt body seem accurately imaged in both cases, especially on the left-hand side where the chalk layer bends upwards. However, common-azimuth migration produces a result significantly more accurate for the top of salt and for the complex lithologic interfaces in that area. Moreover, the reflector marked "S", which may correspond to the salt boundary, is not visible in the PAPsDM image. The PAPsDM migrated section could probably be improved by using a larger offset range in the cross-line direction (700m here). Interestingly enough, handling multiple arrivals does not yield a significantly better image, since the result of 3-D PAPsDM with, respectively, first, strongest, and multiple arrival are similar at 97% (Gilles Lambaré, personal communication).

CONCLUSION

Real data offers an opportunity to test our imaging techniques further. Common-azimuth migration is an attractive method for seismic imaging in complex media and remains a subject for further research. Its computational cost, illustrated in this particular example, can make it an attractive alternative to widespread Kirchhoff methods. The imaging of the North Sea

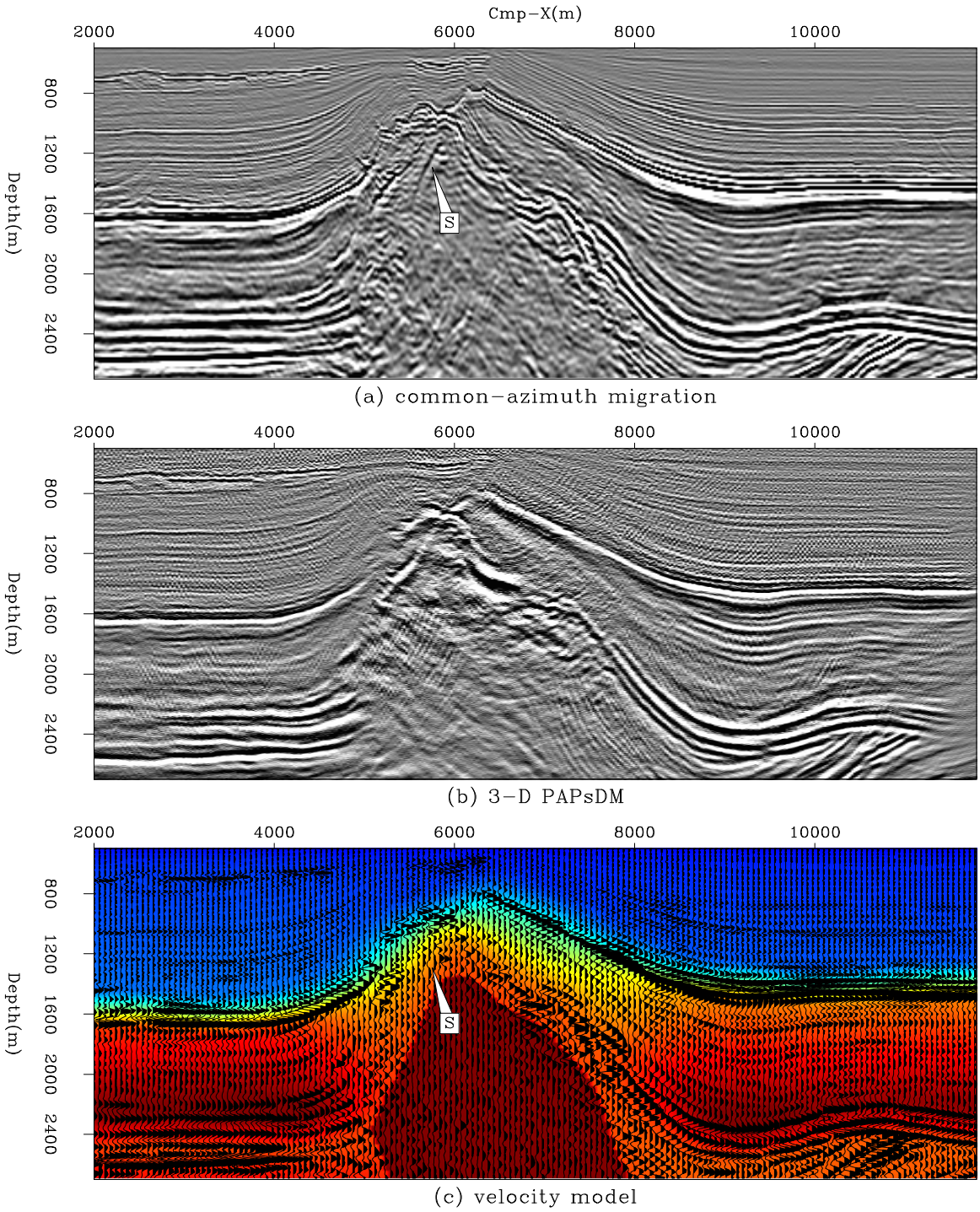

Figure 8: Comparison between the sections at Cmp-X=4100m migrated using 3-D prestack common-azimuth migration (a) and 3-D PAPsDM (b). The third section (c) shows the common-azimuth migrated image superimposed on the velocity model. The PAPsDM result is courtesy of the Ecole des Mines de Paris. louis1-L7d-ComAz-vs-PAPsDM [CR]

data reveals lithologic structures focused with high resolution. Angle-domain common-image gathers highlight imaging insufficiences around the steepest parts of salt flanks. They also offer opportunities for residual migration and velocity estimation. An extended migration scheme, which incorporates a wider range of data in the cross-line direction to account for lateral velocity variations, is being examined (Vaillant and Biondi, 1999).

ACKNOWLEDGEMENTS

The authors would like to thank Elf Aquitaine for providing the data and the velocity model and the research group of the Ecole des Mines de Paris for sharing their results with us. Sincere thanks to Bob Clapp as well, who concurrently developed an upgraded version of SEPlib3D that can now handle huge 3-D datasets and made this study possible. We would like to acknowledge Biondo Biondi for his useful comments and stimulating discussions.

REFERENCES

Biondi, B., and Palacharla, G., 1996, 3-D prestack migration of common-azimuth data: Geophysics, **61**, no. 6, 1822–1832.

Biondi, B., and Sava, P., 1999, Wave-equation migration velocity analysis: SEP–**100**, 11–34.

Biondi, B., Fomel, S., and Chemingui, N., 1998, Azimuth moveout for 3-D prestack imaging: Geophysics, **63**, no. 2, 574–588.

Biondi, B., 1997, Azimuth moveout + common-azimuth migration: Cost-effective prestack depth imaging of marine data: 67th Annual Internat. Mtg., Soc. Expl. Geophys., Expanded Abstracts, 1375–1378.

Ehinger, A., and Lailly, P., 1995, Velocity model determination by the SMART method, part 1: Theory: 65th Annual Internat. Mtg., Soc. Expl. Geophys., Expanded Abstracts, 739–742.

Jacobs, J. A. C., Delprat-Jannaud, F., Ehinger, A., and Lailly, P., 1992, Sequential migration-aided reflection tomography: A tool for imaging complex structures: 62nd Annual Internat. Mtg., Soc. Expl. Geophys., Expanded Abstracts, 1054–1057.

Malcotti, H., and Biondi, B., 1998, Accurate linear interpolation in the extended split-step migration: SEP–**97**, 61–72.

Mosher, C. C., Foster, D. J., and Hassanzadeh, S., 1997, Common angle imaging with offset plane waves: 67th Annual Internat. Mtg., Soc. Expl. Geophys., Expanded Abstracts, 1379–1382.

O'Brien, M. J., and Etgen, J. T., 1998, Wavefield imaging of complex structures with sparse point-receiver data: 68th Annual Internat. Mtg., Soc. Expl. Geophys., Expanded Abstracts, 1365–1368.

Ogilvie, J. S., and Purnell, G. W., 1996, Effects of salt-related mode conversions on subsalt prospecting: Geophysics, **61**, no. 2, 331–348.

Prucha, M. L., Clapp, R. G., and Biondi, B. L., 1998, Imaging under the edges of salt bodies: Analysis of an Elf North Sea dataset: SEP–**97**, 35–44.

Prucha, M. L., Biondi, B. L., and Symes, W. W., 1999, Angle-domain common image gathers by wave-equation migration: SEP–**100**, 101–112.

Sava, P., 1999, Enhancing common-image gathers with prestack stolt residual migration: SEP–**102**, 47–60.

Stoffa, P. L., Fokkema, J. T., de Luna Freire, R. M., and Kessinger, W. P., 1990, Split-step Fourier migration: Geophysics, **55**, no. 4, 410–421.

Thierry, P., Lambaré, G., Podvin, P., and Noble, M., 1999a, 3-D preserved amplitude prestack depth migration on a workstation: Geophysics, **64**, no. 1, 222–229.

Thierry, P., Operto, S., and Lambaré, G., 1999b, Fast 2-D ray+Born migration/inversion in complex media: Geophysics, **64**, no. 1, 162–181.

Vaillant, L., and Biondi, B., 1999, Extending common-azimuth migration: SEP–**100**, 125–134.

Xu, S., Thierry, P., and Lambaré, G., 1999, 3-D migration/inversion in complex media: 69th Annual Internat. Mtg., Soc. Expl. Geophys., Expanded Abstracts, to be presented.